



# Additive-free aerobic oxidative dehydrogenation of N-heterocycles under catalysis by NiMn layered hydroxide compounds



Weyou Zhou<sup>a</sup>, Qianyun Tao<sup>a</sup>, Fu'an Sun<sup>a</sup>, Xinbai Cao<sup>a</sup>, Junfeng Qian<sup>a</sup>, Jie Xu<sup>a</sup>, Mingyang He<sup>a,\*</sup>, Qun Chen<sup>a</sup>, Jianliang Xiao<sup>b</sup>

<sup>a</sup> Jiangsu Key Laboratory of Advanced Catalytic Materials and Technology, Changzhou University, Changzhou 213164, China

<sup>b</sup> Department of Chemistry, University of Liverpool, Liverpool L69 7ZD, United Kingdom

## ARTICLE INFO

### Article history:

Received 27 October 2017

Revised 24 January 2018

Accepted 29 January 2018

Available online 3 March 2018

### Keywords:

Layered hydroxide compounds

Oxidative dehydrogenation

N-heterocycles

Synergistic effect

Heterogeneous catalysis

## ABSTRACT

NiMn layered hydroxide compounds have been found to be efficient catalysts for the oxidative dehydrogenation of N-heterocycles by molecular oxygen under mild conditions. Various tetrahydroquinoline derivatives and some other N-heterocycles have been found to be tolerated by the catalytic system. A synergistic effect between Ni and Mn has been observed in the reaction. A kinetic study concluded that the dehydrogenation of 1,2,3,4-tetrahydroquinoline is a first-order reaction, and an apparent activation energy of 113 kJ/mol has been obtained. A probable reaction mechanism comprising an imine intermediate has been proposed according to the obtained results and XPS analysis. The key catalytic site for the dehydrogenation is thought to be Mn<sup>3+</sup>, which could be stabilized by Ni<sup>2+</sup> in the hydrotalcite structure.

© 2018 Elsevier Inc. All rights reserved.

## 1. Introduction

Dehydrogenation is an important procedure for accessing N-containing heterocycle compounds, which are common intermediates in pharmaceutical and biological active molecules. Up to now, various homogeneous catalysts originated from the metal complexes or salts of Ir [1–4], Ru [5], Fe [6,7], Rh [8], Pd [9,10], Cu [11], and Co [12–14] have been reported for transformation in the presence or absence of an acceptor. *o*-Quinone has also been found effective by Stahl [15] in the dehydrogenation. However, homogeneous systems make it complicated to separate the catalyst and purify the product, and it is hard to achieve high catalytic efficiency, sustainability, and cost-effectiveness.

In this context, heterogeneous catalysts are very attractive for their advantages of reusability, low cost, and simple process. Some heterogeneous catalysts, including supported Ru [16–18], FeO<sub>x</sub>@NGr–C (modified iron oxide nanoparticles loaded on carbon) [19], RhCNT/TBC (carbon-nanotube-anchored rhodium nanoparticles/4-tert-butylcatechol) [20], Cu(0)/Al<sub>2</sub>O<sub>3</sub> [21], Cu/TiO<sub>2</sub> [22], Co<sub>3</sub>O<sub>4</sub>-NGr/C/K<sub>2</sub>CO<sub>3</sub> [23], PdHAP (hydroxyapatite-bound Pd catalyst) [24], AuNPs/C (graphite-supported gold nanoparticles)/NaHCO<sub>3</sub> [25], and Pt nanowire [26], have been prepared and investigated in the dehydrogenation of N-heterocycles. However, noble

metals, additives, or harsh conditions were always required for these catalytic systems, and sometimes complicated methods have to be applied to prepare the catalysts. The establishment of an efficient heterogeneous catalytic system based on readily available materials is highly desirable in view of the principles of practical chemistry. Mesoporous manganese oxide as a heterogeneous catalyst has been found by Suib and co-workers to be feasible for aerobic oxidative dehydrogenation under relatively mild reaction conditions [27]. However, the catalytic system suffered from low efficiency and the limited scope of substrates. Very recently, Gong et al. reported that graphene oxide (GO) could be applied as a catalyst in the transformation [28], but a considerable amount of Na<sub>2</sub>CO<sub>3</sub> was required as an additive. Moreover, the catalytic efficiency and the selectivity of the aromatic products was not very satisfied.

In the course of our study on the development of efficient catalysts for aerobic oxidation, layered hydroxide compounds (LDHs) have shown outstanding activity in the catalytic transformation of alcohols to carbonyl compounds [29,30]. Actually, the LDHs have a great application potential because of the adjustability of their composition and physicochemical properties [31–34]. Furthermore, these compounds can be conveniently prepared in large quantities from commercially available materials [35,36]. These features of LDHs inspired us to further investigate their catalytic performance in the oxidative dehydrogenation of N-containing heterocycle compounds. In the literature, hydrotalcites are mainly used as catalysts or supports in the dehydrogenation of alcohols

\* Corresponding author.

E-mail address: [hemy\\_cczu@126.com](mailto:hemy_cczu@126.com) (M. He).

[37,38], cyclohexane [39], and ethylbenzene [40,41]. Recently, a Ni–Mg–Al layered triple-hydroxide-supported Pd catalyst has been found to be effective in the acceptorless dehydrogenative aromatization of cyclohexanols/cyclohexanones and cyclohexylamines to the corresponding phenols and anilines [42]. To the best of our knowledge, there is no report of the hydrotalcites being used in the dehydrogenation of N-heterocycles.

Initially, various LDHs consisting of different cations were tested in the aerobic dehydrogenation of 1,2,3,4-tetrahydroquinoline. The results in Table S1 in the Supplementary Material show that the conversion of the substrate was higher under the catalysis of the samples containing Cu, Co, or Mn. On the other hand, the selectivity to quinoline was low for most of these samples, except Ni<sub>2</sub>Co and Ni<sub>2</sub>Mn LDHs, with the latter being slightly more selective. On the basis of this preliminary study, a series of NiMn LDHs with different Ni/Mn ratios were synthesized, characterized, and studied in the oxidative dehydrogenation of N-heterocycles by molecular oxygen. The synergistic effect between the Ni and Mn cations, kinetic analysis, and the reaction mechanism are also discussed.

## 2. Experimental

### 2.1. Chemicals and reagents

All the reagents and solvents in the study were analytically pure and were purchased from Energy or Aladdin and used as received. Some N-heterocycles, including 3-methyl-1,2,3,4-tetrahydroquinoline, 4-methyl-1,2,3,4-tetrahydroquinoline, 7-methyl-1,2,3,4-tetrahydroquinoline, 8-methyl-1,2,3,4-tetrahydroquinoline, 6-methoxyl-1,2,3,4-tetrahydroquinoline, 6-fluoro-1,2,3,4-tetrahydroquinoline, 6-chloro-1,2,3,4-tetrahydroquinoline, 2-phenyl-1,2,3,4-tetrahydroquinoline, and 2,3-dimethyl-1,2,3,4-tetrahydroquinoline, were prepared by the reduction of corresponding precursors using NaBH<sub>4</sub> (AR) as a reductant [43]. Other substrates (98–99% purity) were also purchased from Energy or Aladdin and used as received.

### 2.2. General procedure for the preparation of layered hydroxide compounds

All the LDH samples in the present research were prepared through a co-precipitation method. Taking Ni<sub>2</sub>Mn-LDH as an example, 0.04 mol (11.63 g) of Ni(NO<sub>3</sub>)<sub>2</sub>·6H<sub>2</sub>O and 0.02 mol (2.52 g) of MnCl<sub>2</sub> were dissolved in 100 mL deionized water to prepare solution A; and 0.04 mol (1.6 g) of NaOH and 2.8 g of NH<sub>3</sub>·H<sub>2</sub>O (25–28%) were dissolved in 100 mL deionized water to form solution B. Then solution A was added dropwise with stirring (350 rpm) to solution B at 30 °C. After the resulting solutions were digested at 80 °C for 24 h, the resulting precipitate was washed to neutrality with deionized water. The residue was then dried at 120 °C for 12 h to give a powdery Ni<sub>2</sub>Mn-LDH sample. Other samples with different cations and Ni/Mn ratios were obtained by similar procedures.

### 2.3. Characterization of NiMn layered hydroxide compounds

Powder X-ray diffraction (XRD) patterns of the NiMn LDHs were collected on a Rigaku D/max 2500 PC X-ray diffractometer. The content of Ni and Mn was obtained via inductively coupled plasma analysis (ICP) in a Varian Vista-AX device. FTIR spectroscopy and scanning electron microscopy (SEM) were carried out on a Nicolet PROTÉGÉ 460 FTIR spectrometer and a JEOL JSM-6360LA scanning electron microscope, respectively. Thermogravimetric measurements and N<sub>2</sub> adsorption/desorption studies of these compounds were performed in a Seiko Instrument TG/DTA Model 32 and a Micromeritics ASAP2010C apparatus, respectively. A Thermo Sci-

entific ESCALAB 250Xi instrument was used for X-ray photoelectron spectroscopy (XPS) measurements with an incident radiation of nonmonochromatized MgK $\alpha$  X-rays (50 eV) at an electron takeoff angle of 60°.

### 2.4. Aerobic dehydrogenation of 1,2,3,4-tetrahydroquinoline

Typically, a mixture of 1,2,3,4-tetrahydroquinoline (0.50 mmol), Ni<sub>2</sub>Mn-LDH (80 mg), and mesitylene (2 mL) in a carousel reaction tube was magnetically stirred at 120 °C under 1 atm of oxygen. The reaction was monitored and analyzed through a gas chromatograph (Shimadzu GC-2010AF) with a flame ionization detector (FID). After completion of the reaction, the reaction mixture was cooled and separated by filtration to recycle the catalyst. After being washed with solvent and dried at 120 °C for 12 h, the recycled catalyst was reused under similar conditions. The conversion of the substrate and the selectivity of quinoline were obtained on the basis of GC analysis (chlorobenzene was used as the internal standard reference). The quasi-turnover frequency (qTOF) value was calculated on the basis of the GC analysis and Mn content in the catalyst with a conversion lower than 10%. The conversion, selectivity, and qTOF are defined as follows:

$$\text{Conversion(\%)} = \frac{\text{moles of reactant converted}}{\text{moles of reactant in feed}} \times 100\%$$

$$\text{Selectivity(\%)} = \frac{\text{moles of product formed}}{\text{moles of reactant converted}} \times 100\%$$

$$\text{qTOF(h}^{-1}\text{)} = \frac{\text{moles of reactant converted}}{\text{moles of total active sites} \times \text{reaction time}}$$

### 2.5. Catalytic dehydrogenation of other N-heterocyclic amines

A mixture of N-heterocyclic amine (0.50 mmol), Ni<sub>2</sub>Mn-LDH (80 mg), and mesitylene or DMF (2 mL) in a carousel reaction tube was stirred at 120 °C under 1 atm oxygen. After the completion of the reaction, monitored by TLC (thin-layer chromatography, petroleum ether/ethyl acetate 10:1 (v/v)), the mixture was cooled and purified using flash chromatography to give the corresponding product. NMR spectra were recorded on a Bruker ADVANCE 400-NMR spectrometer (400 MHz). Silica gel 60 F254 thin-layer chromatography plates (Sinopharm) was used for thin-layer chromatography with petroleum ether/ethyl acetate (10:1 v/v) as the mobile phase.

## 3. Results and discussion

### 3.1. Characterization of NiMn layered hydroxide compounds

Characteristic LDH reflections for all the Ni<sub>x</sub>Mn-LDHs can be observed from the powder XRD patterns depicted in Fig. 1. The sharp and symmetrical peaks at about 11° and 22° can be assigned to the (0 0 3) and (0 0 6) planes, respectively; the broad and asymmetrical peaks observed between 33° and 47° are for the (0 1 2), (0 1 5), and (0 1 8) planes [44–46]. The results indicate that some amount of Mn<sup>2+</sup> was oxidized to Mn<sup>3+</sup> during the preparation, because trivalent cations are essential for the formation of the hydrotalcite structure [47,48]. Actually, Mn<sup>4+</sup> was also formed during the co-precipitation, because both Mn<sup>3+</sup> and Mn<sup>4+</sup> were found through the XPS analysis (Section 3.4). Therefore, a possible oxidation path from Mn<sup>2+</sup> to Mn<sup>3+</sup> and Mn<sup>4+</sup> was proposed (Scheme 1) concerning the alkaline environment during the preparation of NiMn hydrotalcites. It can be observed from the reflections related to the planes (1 1 0) and (1 1 3) that the crystallinity decreases with the increase of Ni/Mn ratio [49,50]. About 7.94 Å was

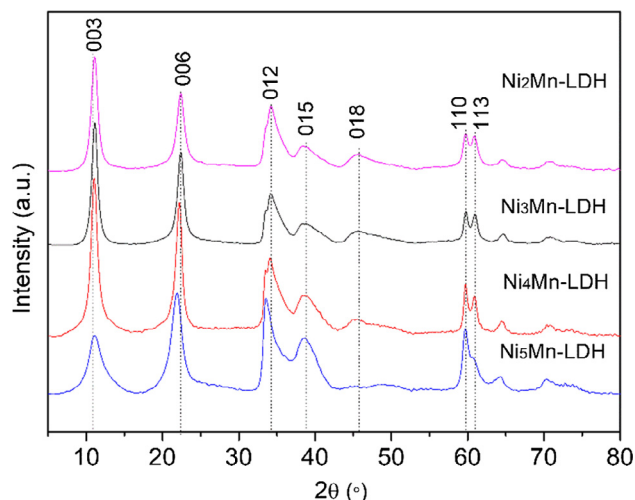


Fig. 1. The XRD patterns of  $Ni_xMn$ -LDH samples.



Scheme 1. The possible oxidation path of  $Mn^{2+}$  to  $Mn^{3+}$  and  $Mn^{4+}$ .

obtained for the basal spacings of  $Ni_xMn$ -LDHs by calculating from the (0 0 3) reflection, suggesting that the main anions in the interlayers of all the samples were mainly  $OH^-$  and  $CO_3^{2-}$  [51]. Further, the FTIR spectra (Fig. S2 in the Supplementary Material), TG-DTG curves of  $Ni_xMn$ -LDHs (Fig. S3), and SEM image (Fig. S4) indicate that hydrotalcite structures were formed for all the samples. The Ni/Mn ratios were also consistent with the theoretical values from ICP analysis (Table 1).

$N_2$  adsorption/desorption measurement was performed to explore the textural parameters of the NiMn hydrotalcites (Table 1 and Fig. S5). The analysis results indicate that the BET surface area of these samples changes irregularly, while the pore volumes and the average pore diameters of these NiMn LDHs decrease with the increase of the Ni/Mn ratio. Compared with the common NiAl LDH [29], the pore volumes and average pore diameter increase when Al is replaced with Mn in hydrotalcites. These phenomena might be due to the change of the microscopic morphology for the different cations in the brucite layer [52,53].

## 3.2. Catalytic activity of NiMn layered hydroxide compounds

### 3.2.1. Optimization of the reaction conditions

First, dehydrogenation of 1,2,3,4-tetrahydroquinoline was selected as a model reaction using  $Ni_2Mn$ -LDH as a catalyst to optimize the reaction conditions. Concerning the solvent, the results summarized in Table 2 show that both polar and nonpolar solvents gave higher conversions, while much lower activity was observed in the solvents with medium polarity. Almost full conversion of

Table 2  
Optimization of the reaction conditions:

Entry	Catalyst	Solvent	Conv./% <sup>b</sup>	Sel./% <sup>b</sup>
1	$Ni_2Mn$ -LDH	DMF	90	85
2	$Ni_2Mn$ -LDH	DMSO	76	74
3	$Ni_2Mn$ -LDH	Acetonitrile	29	20
4	$Ni_2Mn$ -LDH	Mesitylene	>99	86
5	$Ni_2Mn$ -LDH	Dioxane	26	18
6	$Ni_2Mn$ -LDH	Benzotrifluoride	82	73
7	$Ni_2Mn$ -LDH	Benzonitrile	96	78

<sup>a</sup> Reaction conditions: 1,2,3,4-tetrahydroquinoline 0.5 mmol, catalyst 100 mg, temperature 100 °C, reaction time 12 h, solvent 2 mL, under oxygen.

<sup>b</sup> Based on GC analysis. The by-products were not quantified.

1,2,3,4-tetrahydroquinoline and high selectivity to quinoline were observed in mesitylene. Although comparable selectivity was obtained under DMF (N,N-dimethylformamide), the conversion was slightly lower. These results suggest that a nonpolar solvent could provide higher reactivity for dehydrogenation.

For the reaction temperature, it is found that the reaction rate markedly increased at higher temperature, and the dehydrogenation could finish in 1.5 h at 140 °C. However, the highest selectivity and yield of the corresponding product were obtained at 120 °C with a reaction time of 2 h (Fig. 2). A higher reaction temperature and prolonged reaction time would result in the formation of overoxidation product and decrease of the selectivity.

The amount of catalyst was optimized under the selected conditions (Fig. S6). The yield of quinoline was highest, with almost complete conversion, when 80 mg of  $Ni_2Mn$ -LDH was used for 0.5 mmol of substrate. Further increasing the amount of catalyst resulted in deep oxidation and reduction of the selectivity. Finally, the catalytic activities of these  $Ni_xMn$  LDHs with different Ni/Mn ratios were compared under optimized conditions. The results in Fig. 3 and Table 3 show that  $Ni_2Mn$ -LDH exhibited the highest conversion and selectivity, although  $Ni_4Mn$ -LDH showed the highest qTOF value. The results might be related to the  $S_{BET}$  and the content of Mn, which reached the highest value for  $Ni_2Mn$ -LDH. To check if the surface property affected the catalytic performance, these samples were qualitatively analyzed by testing the pH value of their suspension, which is a general method for analyzing the surface properties of hydrotalcites [29,30]. Weak acidity was observed for the present samples (Table S2). Temperature-programmed desorption of ammonia ( $NH_3$  TPD) is an efficient method for measuring the acidity of samples, but the high temperature needed during the pretreatment must destroy the structure of LDHs samples. Therefore, the number of acidic sites in the catalysts was analyzed qualitatively using Hammett indicators. The results showed that the number of acidic sites decreased as the Ni/Mn ratio increased, but the difference was quite small, suggesting that the surface acidity might have little effect on the catalytic performance.

Table 1  
Sample notation and chemical composition of  $Ni_xMn$ -LDHs.

Sample	Weight content (%)		Ni:Mn	$S_{BET}$ ( $m^2/g$ )	Pore volume ( $cm^3/g$ )	Average pore diameter (nm)
	Ni	Mn				
$Ni_2Mn$ -LDH	35.1	16.1	2.18	124 (47.4) <sup>a</sup>	0.36 (0.09) <sup>a</sup>	11.8 (5.25) <sup>a</sup>
$Ni_3Mn$ -LDH	36.6	11.2	3.26	98	0.26	10.7
$Ni_4Mn$ -LDH	39.6	9.6	3.86	64	0.22	10.3
$Ni_5Mn$ -LDH	42.7	7.9	5.38	98	0.17	7.1

<sup>a</sup> The data in parentheses are for the second recycled sample.

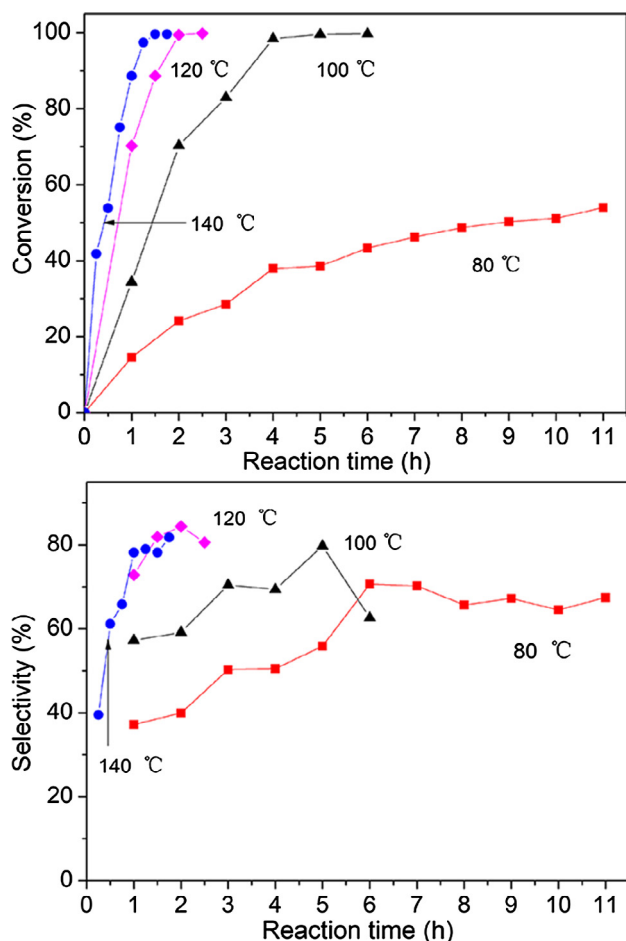


Fig. 2. The effect of temperature on the dehydrogenation. Reaction conditions: 1,2,3,4-tetrahydroquinoline 0.5 mmol, Ni<sub>2</sub>Mn-LDH 100 mg, mesitylene 2 mL, 1 atm oxygen.

Compared with mesoporous manganese oxide (for which the yield was 95%) [27], a comparable yield of dehydrogenation product was obtained. However, the mesoporous manganese oxide system only gave a TON (turnover number) of 1.7 in 20 h, whereas the present catalytic system could present a high qTOF value (43 h<sup>-1</sup>, Table 3, entry 1) under optimized conditions. In conclusion, NiMn LDHs have been developed as an efficient catalyst for the aerobic oxidative dehydrogenation of 1,2,3,4-tetrahydroquinoline.

### 3.2.2. The scope of substrates

With the establishment of optimized conditions, various tetrahydroquinoline derivatives were investigated in the catalytic system (Table 4). When methyl was substituted at the 2-, 3-, or 4-site, the substrates were well tolerated (entries 2–4), and moderate yields were obtained. It should be noted that the reaction performed under DMF could give higher yields of the corresponding dehydrogenated products for the substrates with longer reaction times. These results indicated that mesitylene could provide higher reactivity than DMF in these cases. However, the lower activity of DMF might suppress the formation of the overoxidation products and give better selectivity of the corresponding dehydrogenation products, which could explain the relatively higher yields in DMF. From the reaction time needed for the full conversion of substrates, a steric effect might exist in the transformation, which was also observed in the case of the PdHAP catalytic system [24]. When the aromatic ring was substituted with a methyl or methoxyl

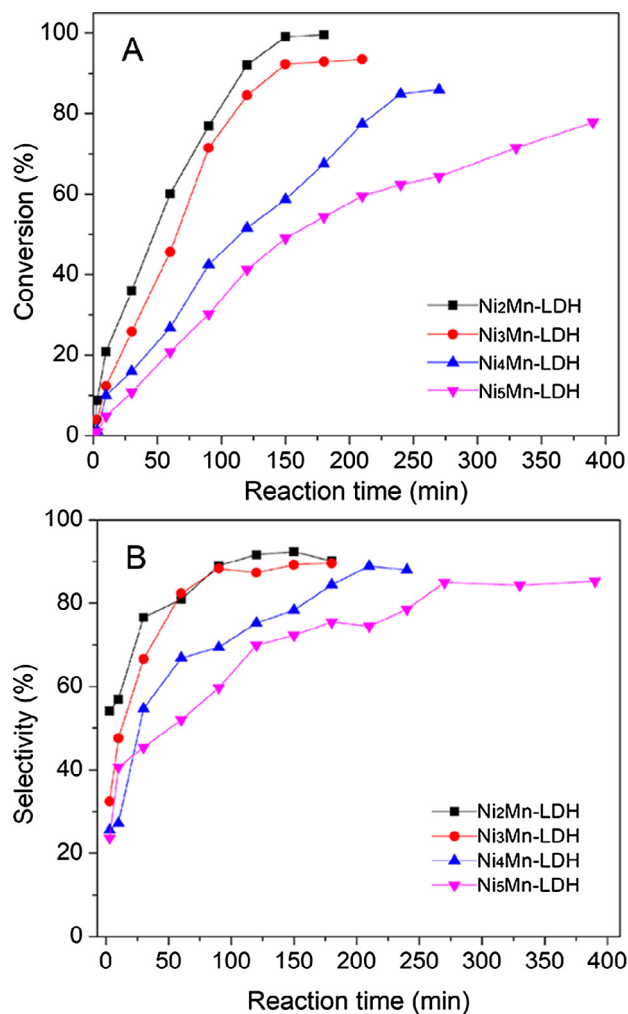


Fig. 3. The catalytic performance of Ni<sub>x</sub>Mn-LDHs (x = 2, 3, 4, 5) in the dehydrogenation. Reaction conditions: 1,2,3,4-tetrahydroquinoline 0.5 mmol, catalyst 80 mg, temperature 120 °C, mesitylene 2 mL, under oxygen.

Table 3  
Comparison of the catalytic activity of Ni<sub>x</sub>Mn-LDHs.<sup>a</sup>

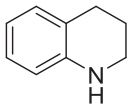
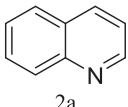
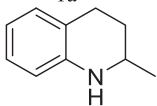
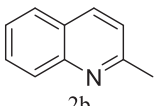
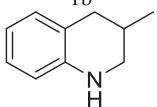
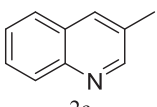
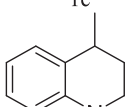
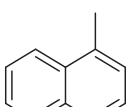
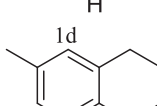
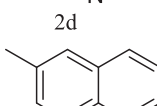
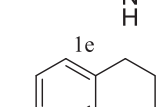
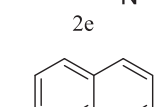
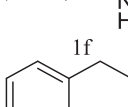
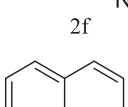
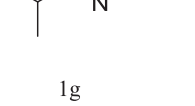
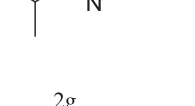
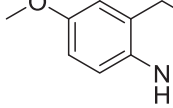
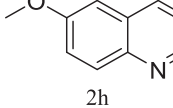
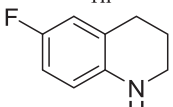
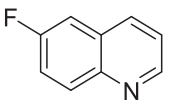
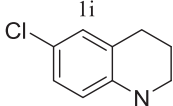
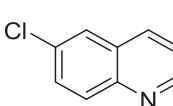
Entry	Catalyst	Conv./% <sup>b</sup>	Sel./% <sup>b</sup>	qTOF/h <sup>-1</sup>
1	Ni <sub>2</sub> Mn-LDH	>99	92	43
2	Ni <sub>3</sub> Mn-LDH	93	89	61
3	Ni <sub>4</sub> Mn-LDH	59	78	71
4	Ni <sub>5</sub> Mn-LDH	49	72	26

<sup>a</sup> Reaction conditions: 1,2,3,4-tetrahydroquinoline 0.5 mmol, catalyst 80 mg, temperature 120 °C, reaction time 2.5 h, mesitylene 2 mL, under oxygen.

<sup>b</sup> Based on the GC analysis.

group, little effect could be observed (entries 5–7). Interestingly, for halogen substituents at the 6 position, bromide gave the highest yield of 88%, while only about 40% yield could be obtained for F and Cl. These results suggest that electronic effect has a significant influence on the reaction. The strong electron-withdrawing groups F and Cl reduce the reactivity of the substrates, which can also be concluded from the reaction time. When Cl was located at an 8 site, an excellent 91% yield of the corresponding product was obtained, indicating that the Cl at the 8 site has lower impact on the reaction than at the 6 site. Interestingly, a phenyl at the 2 position conferred a much higher reactivity on the substrate, which was fully converted in 4 h (entry 13). The observation indicates that the C–H

**Table 4**  
Scope of the oxidative dehydrogenation of tetrahydroquinoline derivatives.<sup>a</sup>

Entry	Substrate	Product	Reaction time/h <sup>b</sup>	Isolated yield/% <sup>b</sup>
1			2.5	85
2			6 (24)	54 (71)
3			8 (24)	53 (66)
4			6.5 (24)	58 (74)
5			4	67
6			4	71
7			3.5	75
8			6	68
9			9.5	39
10			8	44
11			5	88

(continued on next page)



Table 4 (continued)

Entry	Substrate	Product	Reaction time/h <sup>b</sup>	Isolated yield/% <sup>b</sup>
12			4	91
13			4	93
14			9	52
15			7	50
16			7.5	56

<sup>a</sup> Reaction conditions: substrate 0.5 mmol, Ni<sub>2</sub>Mn-LDH 80 mg, temperature 120 °C, mesitylene 2 mL, under oxygen.

<sup>b</sup> The data in brackets were obtained using DMF as the solvent.

bond is activated by the phenyl ring. It is also concluded that the oxidative dehydrogenation reaction is more prone to be affected by electronic effects than by steric hindrance. Moreover, some disubstituted substrates were introduced into the investigation, and moderate yields of the corresponding products were obtained. Compared with 6-bromo-1,2,3,4-tetrahydroquinoline, 6-bromo-2-methyl-1,2,3,4-tetrahydroquinoline gave only a 50% yield, which might be ascribed to the hindrance of the methyl group (entry 15).

The high reactivity of the tetrahydroquinoline derivatives inspired us to explore the applicability of the NiMn LDH catalytic system in other N-containing compounds. The results in Table 5 indicate that the current catalytic system tolerates various N-containing aromatic heterocycles under optimized conditions. The dehydrogenation of 1,2,3,4-tetrahydroquinoxaline and its derivatives gave good results for the corresponding products (entries 1 and 2). A moderate yield of isoquinoline could be obtained in the case of 1,2,3,4-tetrahydroisoquinoline (entry 3). Concerning 2,3-dihydroindole and its substituted variants, an electro-withdrawing group benefited the dehydrogenation, and a high 89% yield was obtained for the 5-nitroindoline (entries 4–6). In the case of N-phenylbenzylamine, a low yield to 4 h (38%) was observed (entry 7), with by-products benzaldehyde and aniline, the formation of which could be ascribed to the oxidative cleavage of the C=N bond [54]. The oxidation of the Hantzsch ester gave the corresponding dehydrogenation product with an excellent yield under a short reaction time (entry 8), which might be due to its strong trend toward a stable aromatic ring.

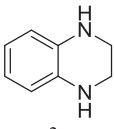
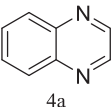
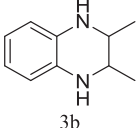
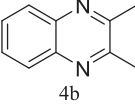
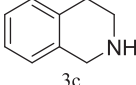
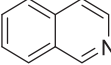
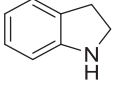
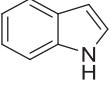
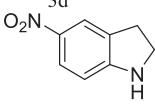
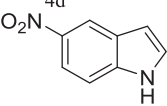
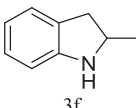
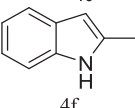
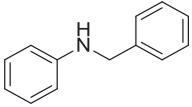
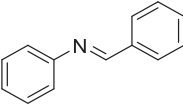
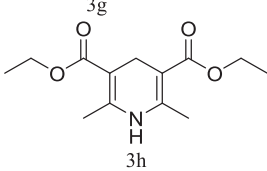
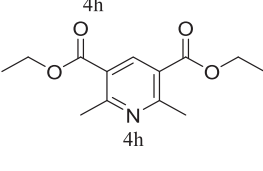
### 3.2.3. The stability and recyclability of the NiMn layered hydroxide compounds

Using 1a as a substrate, a hot filtration experiment was first performed to probe the stability of the catalyst. After 50 min (at about 50% conversion), the filtrate without catalyst was sampled and stirred for the next 70 min; no further conversion of the substrate was

detected (Fig. 4). To further check the leaching of metals, the reaction filtrate and a referential sample were analyzed by ICP. The results showed that the amounts of Ni and Mn ions in the liquid phase of catalytic reaction were only  $111 \times 10^{-9}$  and  $33 \times 10^{-9}$  g/mL, respectively, indicating that no leaching of Ni or Mn ions occurred during the reaction.

The recyclability of Ni<sub>2</sub>Mn-LDH has also been studied. The results (Fig. S7) indicate that a prolonged time was required to obtain results similar to those for the fresh Ni<sub>2</sub>Mn-LDH. The catalytic activity decreased significantly after reuse for three times; therefore XRD was used to monitor the change of recycled samples. The XRD patterns shown in Fig. S8 confirm that the hydrotalcite structure was retained after multiple recycles, but the crystallinity significantly decreases concerning the reflections related to the planes (1 1 0) and (1 1 3) [49,50]. The lattice parameters *a* and *c* were calculated from the peaks associated with planes (1 1 0) and (0 0 3) assuming a 3R stacking sequence (Table S3). Parameter *a* ( $=2d_{110}$ ) is a function of cation–cation distance in the hydrotalcite layer, which reflects the density of metal ion stacking in the (1 1 0) plane [55,56]. The variation tendency mainly depends on the cation size. In the present study, no significant change of the *a* value was observed for the recycled samples, because only Ni and Mn cations existed in the structure of NiMn LDHs. On the other hand, the value of parameter *c* ( $=(3d_{003} + 6d_{006})/2$ ) is the thickness of one hydrotalcite layer and one interlayer [55–57]. It is regulated by several factors such as the water content in the interlayer, the size of anions between the brucite layers, the cations, and electrostatic interaction between anions and positively charged brucite-like sheets [55,58]. For the recycled Ni<sub>2</sub>Mn-LDH samples, the *c* value increased from 23.785 to 24.542 Å. The results might be ascribed to the fact that electrostatic interaction between anions and brucite-like sheets was weakened after recycling, because other factors were all similar. Further, the decline was probably due to the variation of valence of Mn cations; i.e., the proportion

**Table 5**  
Oxidative dehydrogenation of other N-containing compounds under Ni<sub>2</sub>Mn-LDH.<sup>a</sup>

Entry	Substrate	Product	Reaction time/h <sup>b</sup>	Isolated yield/% <sup>b</sup>
1		 4a	9	69
2		 4b	6	79
3		 4c	6.5	51
4		 4d	8.5	45
5		 4e	15	89
6		 4f	20	31
7			24	38 <sup>b</sup>
8		 4h	5	92

<sup>a</sup> Reaction conditions: substrate 0.5 mmol, Ni<sub>2</sub>Mn-LDH 80 mg, temperature 120 °C, mesitylene 2 mL, under oxygen.

<sup>b</sup> Based on GC analysis.

of Mn cations with high valences decreased. The ratio of Mn<sup>2+</sup>/Mn<sup>3+</sup>/Mn<sup>4+</sup> could be estimated through XPS analysis results (Section 3.4), and it changed from 1/9.5/2.9 to 1/3.6/2.8, indicating that the proportion of Mn<sup>3+</sup> decreased significantly after the reaction. As a result, the catalytic activity of the recycled Ni<sub>2</sub>Mn-LDH decreased, because Mn<sup>3+</sup> was thought to be the more active site (discussed in Section 3.4).

Next, N<sub>2</sub> adsorption/desorption measurement was performed to explore the change of the textural parameters of recycled Ni<sub>2</sub>Mn-LDH. The S<sub>BET</sub>, pore volume, and average pore diameter were all significantly decreased after the second recycle (Table 1), suggesting that collapse and shrinkage of the NiMn hydrotalcite occurred during the catalytic reaction. The change in textural parameters might also be responsible for the deactivation of the catalyst.

### 3.3. Kinetic study

Prior to the kinetic study, the existence of pore diffusion limitations inside the catalysts and the external diffusion effect were examined. For the internal diffusion, a Weisz–Prater criterion was applied in the catalytic system [59–61]:

$$\phi_{WP} = \frac{r_a R_p^2}{C_s D_{eff}} \quad (1)$$

The calculation was performed according to Ref. [60] for a similar liquid-phase reaction, and the detailed calculation procedure can be found in the Supplementary Material. The value of  $\phi_{WP}$  for each reactant ( $\phi_{WP|O_2} = 1.458 \times 10^{-2}$ ,  $\phi_{WP|tetrahydroquinolin} = 3.879 \times 10^{-4}$ ) is less than 0.3, which excludes the significant pore diffusional limitations during the oxidative dehydrogenation of 1,2,3,4-tetrahydroquinoline in mesitylene under the selected conditions [60]. Further, the external diffusion effect was tested by adjusting the rotational speed (Fig. S9). The results show that external diffusion could be neglected when the rotational speed was higher than 150 rpm in the catalytic reaction.

The kinetic aspects of the reaction were studied by performing time-dependent experiments at different temperatures (Fig. 5). The results indicated that the dehydrogenation of 1,2,3,4-tetrahydroquinoline is a first-order reaction, consistent with the result for mesoporous manganese oxide catalyst [27].

For the experiments performed at different temperatures,  $k$  values can be correlated by an Arrhenius-type expression. The parameters of the Arrhenius equation,

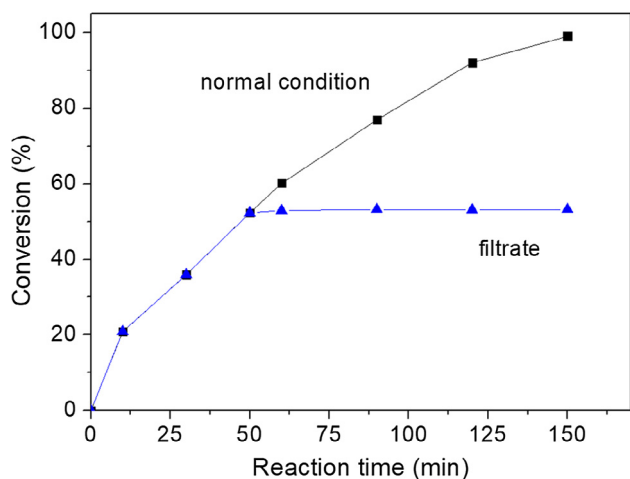


Fig. 4. Hot filtration test. Reaction conditions: 1,2,3,4-tetrahydroquinoline 0.5 mmol, Ni<sub>2</sub>Mn-LDH 80 mg, temperature 120 °C, mesitylene 2 mL, under oxygen.

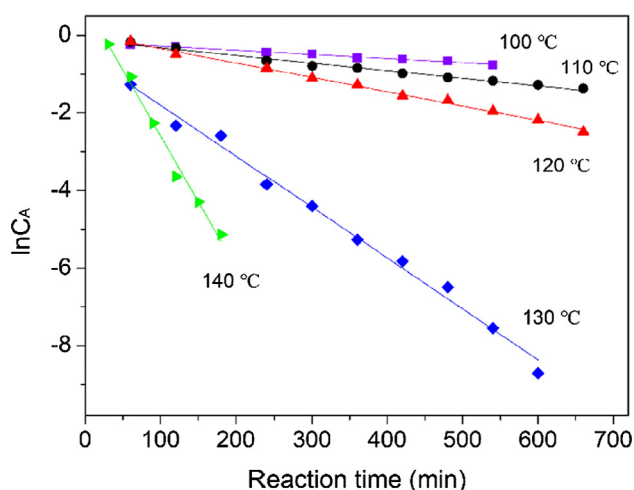


Fig. 5. First-order kinetics fit of dehydrogenation of 1,2,3,4-tetrahydroquinoline. Reaction conditions: 1,2,3,4-tetrahydroquinoline 2 mmol, Ni<sub>2</sub>Mn-LDH 160 mg, mesitylene 2 mL, under oxygen.

$$\ln k = \ln A_0 - \frac{E_a}{RT} \quad (2)$$

where  $E_a$  is the energy of activation (kJ/mol) and  $A_0$  is the pre-exponential factor ( $\text{min}^{-1}$ ), can be deduced via the plot of  $\ln k$  to the  $1/T$  depicted in Fig. 6.

A multiple regression analysis for the constants in Fig. 6 against temperature with this expression led to a value of 113 kJ/mol for the apparent activation energy ( $E_a$ ). The value was higher than that obtained in the case of mesoporous manganese oxide catalyst ( $8.3 \pm 0.2$  kcal/mol) [27], but the present catalytic system exhibited a higher reaction rate and better results under the selected conditions.

### 3.4. Discussion of the synergy and mechanism

To gain further insight into the high activity of the NiMn LDHs, some controlled experiments were performed (Table 6). Only a trace of the substrate was transformed without catalyst, implying that the catalyst was critical for the transformation of 1,2,3,4-tetrahydroquinoline (entry 2). When the catalytic dehydrogenation was performed under nitrogen, the substrate could be transformed in a moderate conversion with reduced selectivity (entry 3), which

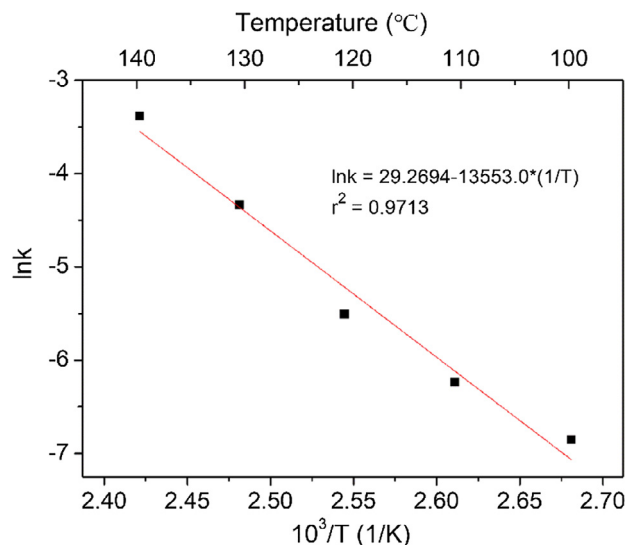


Fig. 6. Arrhenius plot for the oxidative dehydrogenation of 1,2,3,4-tetrahydroquinoline by Ni<sub>2</sub>Mn-LDH.

Table 6  
Some controlled experiments.<sup>a</sup>

Entry	Catalyst	Additive	Conv./%	Sel./%
1	Ni <sub>2</sub> Mn-LDH	–	>99	92
2	–	–	trace	–
3 <sup>b</sup>	Ni <sub>2</sub> Mn-LDH	–	64	83
4	Mg <sub>2</sub> Mn-LDH	–	70	23
5	Ni <sub>2</sub> Al-LDH	–	8	67
6	Ni <sub>2</sub> Mn-LDH	BHT <sup>c</sup>	96	39
7	Ni <sub>2</sub> Mn-LDH	TEMPO <sup>c</sup>	93	97
8	Ni <sub>2</sub> Mn-LDH	CCl <sub>3</sub> Br <sup>c</sup>	49	54
9	Activated MnO <sub>2</sub>	–	49	68

<sup>a</sup> Reaction conditions: 1,2,3,4-tetrahydroquinoline 0.5 mmol, catalyst 80 mg, temperature 120 °C, reaction time 2.5 h, mesitylene 2 mL, under oxygen atmosphere.

<sup>b</sup> Under nitrogen.

<sup>c</sup> Two equivalents of substrate.

might be due to the limited number of lattice oxygens of Ni<sub>2</sub>Mn-LDH [27].

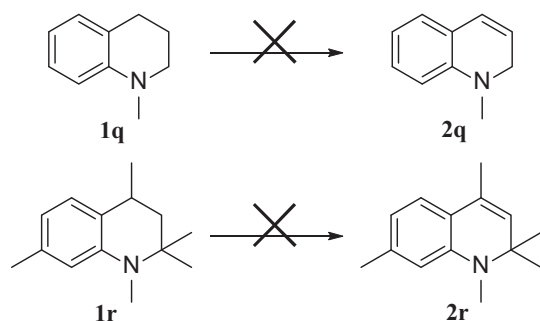
Further, the preparation of Mg<sub>2</sub>Mn-LDH and Ni<sub>2</sub>Al-LDH was tried according to a similar method to discuss the possible synergistic effect between the Ni and Mn cations in the catalytic dehydrogenation, considering that Mg and Al are the most common components of hydrotalcites. The XRD patterns of the two samples depicted in Fig. S10 show that a hydrotalcite structure was formed for Ni<sub>2</sub>Al-LDH, whereas the Mg<sub>2</sub>Mn sample could not give a pure hydrotalcite structure. It is well known that M<sup>2+</sup> and M<sup>3+</sup> cations are normal components of hydrotalcite. However, high spin Mn<sup>3+</sup> *d*4 ions are susceptible to Jahn–Teller distortions. Jayashree et al. have reported that Ni<sup>2+</sup> can stabilize the Mn<sup>3+</sup> cations in the hydrotalcite structure through hybridization of the Mn(3*d*) orbitals with the Ni(3*d*) orbitals to yield an average *d* electron configuration per metal atom greater than 4 [62]. Therefore, the impure crystal formed for Mg<sub>2</sub>Mn sample might be due to the fact that Mg<sup>2+</sup> does not have the ability to stabilize Mn<sup>3+</sup>. Then the two samples were investigated in the oxidative dehydrogenation of the 1,2,3,4-tetrahydroquinoline. Interestingly, a marked decrease of conversion and selectivity was observed for the two samples (Table 6, entries 4 and 5), suggesting that synergy might exist between the Ni and Mn components.

A series of controlled experiments were conducted to get further understanding of the reaction mechanism for the catalytic



dehydrogenation. To examine the possibility of a radical reaction pathway, BHT (2,6-di-tert-butyl-4-methylphenol), TEMPO (2,2,6,6-tetramethylpiperidine-1-oxyl), and  $\text{CCl}_3\text{Br}$  as radical scavengers were introduced into the catalytic system. It could be observed that these radical scavengers suppressed the reaction to some extent, while the selectivity decreased significantly in the presence of BHT or  $\text{CCl}_3\text{Br}$  (Table 6, entries 6–8). These phenomena indicate that radical intermediate might form in the reaction.

In addition, when N-methyl-1,2,3,4-tetrahydroquinoline (1q) was applied as the substrate (Scheme 2), no dehydrogenation product could be detected and almost 100% recovery could be obtained based on GC analysis. The results suggested that the presence of the N–H proton is critical for the dehydrogenation to



Scheme 2. Control experiments to show the importance of the N–H moiety.

proceed. On the other hand, the reaction with 2,2,4,7-tetramethyl-1,2,3,4-tetrahydroquinoline (1r) could not result in the corresponding dehydrogenation product (Scheme 2), indicating that imine intermediate might form in the reaction. Furthermore, the results also suggested that the direct formation of a C=C linkage at 3,4-sites is impossible.

XPS was used to determine the surface manganese and nickel valence and their variations. It can be observed from Fig. 7 that the Mn2p region for all the samples contains a spin-orbit doublet with  $\text{Mn}2p_{1/2}$  (653.0 eV) and  $\text{Mn}2p_{3/2}$  (642.5 eV). For the fresh  $\text{Ni}_2\text{-Mn-LDH}$  sample, the  $\text{Mn}2p_{3/2}$  spectrum could be fitted by three peaks at 641.3, 642.5, and 644.6 eV, respectively. According to the reported results [27,63–65], these peaks could be indexed to  $\text{Mn}^{2+}$ ,  $\text{Mn}^{3+}$ , and  $\text{Mn}^{4+}$  cations, respectively. The presence of  $\text{Mn}^{4+}$  may result in some difficulties to form the hydrotalcites; however, there have been a few reports of LDHs that comprise quadrivalent ions in small parts [62]. The content of  $\text{Mn}^{3+}$  in the present sample evidently was the highest (Fig. 7A), consistent with the structure of typical hydrotalcite compounds. When  $\text{Ni}_2\text{-Mn-LDH}$  was used in dehydrogenation under  $\text{N}_2$  atmosphere, the  $\text{Mn}2p$  spectrum of the material (Fig. 7B) showed a valence mixture of  $\text{Mn}^{3+}$  (642.6 eV) and  $\text{Mn}^{2+}$  (640.9 eV), indicating that the redox reaction happened. After the normal catalytic process, the manganese valence recovered (Fig. 7C), suggesting that the catalytic cycle was finished. The  $\text{Ni}2p$  spectra for the studied samples depicted in Fig. S11 show similar spectra. The  $\text{Ni}2p_{3/2}$  ( $\approx 855.8$  eV) and  $\text{Ni}2p_{1/2}$  ( $\approx 873.4$  eV) peaks accompanied by two satellite bands suggest the  $\text{Ni}^{2+}$  states during the reaction [29,66,67], and no valence variation happened

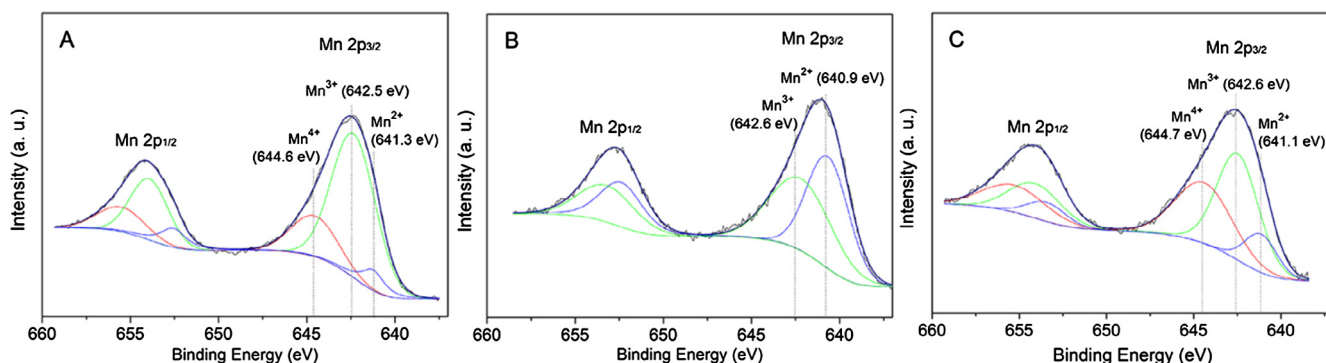
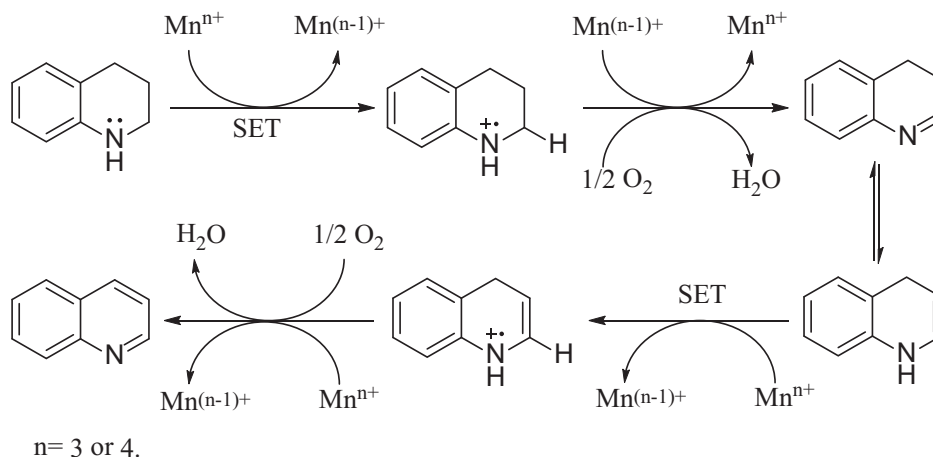


Fig. 7. The Mn2p XPS of  $\text{Ni}_2\text{-Mn-LDH}$  (A) before the reaction; (B) after the reaction under nitrogen; (C) after the reaction under oxygen.



Scheme 3. A possible reaction mechanism for the aerobic oxidation dehydrogenation of 1,2,3,4-tetrahydroquinoline under  $\text{Ni}_2\text{-Mn-LDH}$ .

to nickel cations. These XPS results implied that the dehydrogenative pathway under the catalysis of Ni<sub>2</sub>Mn-LDH includes multielectron transfer between the Mn cations and the substrate. As a comparison, activated MnO<sub>2</sub> was investigated in dehydrogenation under the same conditions. Only about 49% of the 1,2,3,4-tetrahydroquinoline was converted, with markedly lower selectivity (Table 6, entry 9), implying that the Mn<sup>3+</sup> in the LDH structure may play the key role in oxidative dehydrogenation.

Finally, the formation of hydrogen was tested through a GC equipped with a thermal conductivity detector for the catalytic reaction of 1a under N<sub>2</sub>. The results showed that no hydrogen was produced during the reaction, suggesting that H<sub>2</sub>O molecules were formed as the byproduct [19,27].

According to the obtained and reported results [6,19,27], we assume that the dehydrogenation is initiated from single electron transfer (SET) from nitrogen to Mn<sup>4+</sup> or Mn<sup>3+</sup> (Scheme 3). Then the formed amine radical species underwent  $\alpha$  C–H abstraction to afford an imine intermediate with the formation of molecular H<sub>2</sub>O and reoxidation of the reduced manganese. The imine intermediate may be in equilibrium with an enamine. Finally, a new SET from the electron-rich enamine followed by a second C–H abstraction process affords the product. Alternatively, the enamine may act as a hydride donor to reduce a metal-cation-activated imine, which would afford the substrate and product [2,11,68].

#### 4. Conclusions

In conclusion, NiMn hydrotalcites have been found to be an easy-to-manufacture and efficient catalyst for the oxidative dehydrogenation of N-heterocycles by molecular oxygen. The present catalytic system could tolerate various N-containing substrates. A kinetic study concluded that the dehydrogenation of 1,2,3,4-tetrahydroquinoline is a first-order reaction, with an apparent activation energy of 113 kJ/mol. XPS was used to monitor the variation of manganese and nickel valence, and the results suggest that Mn<sup>3+</sup> plays a key role in dehydrogenation. A synergistic effect between Ni and Mn cations was observed; Ni<sup>2+</sup> cations could stabilize Mn<sup>3+</sup> in the hydrotalcite structure. Further, a probable reaction mechanism involving an imine intermediate is proposed according to the results obtained.

#### Acknowledgments

This work was supported by the Advanced Catalysis and Green Manufacturing Collaborative Innovation Center of Changzhou University and the National Science Foundation of China (21403018, 21676030).

#### Appendix A. Supplementary material

Supplementary data associated with this article can be found, in the online version, at <https://doi.org/10.1016/j.jcat.2018.01.030>.

#### References

- [1] Z.H. Wang, I. Tonks, J. Belli, C.M. Jensen, Dehydrogenation of N-ethyl perhydrocarbazole catalyzed by PCP pincer iridium complexes: evaluation of a homogenous hydrogen storage system, *J. Organomet. Chem.* 694 (2009) 2854–2857.
- [2] J.J. Wu, D. Talwar, S. Johnston, M. Yan, J.L. Xiao, Acceptorless dehydrogenation of nitrogen heterocycles with a versatile iridium catalyst, *Angew. Chem. Int. Ed.* 52 (2013) 6983–6987.
- [3] R. Yamaguchi, C. Ikeda, Y. Takahashi, K. Fujita, Homogeneous catalytic system for reversible dehydrogenation–hydrogenation reactions of nitrogen heterocycles with reversible interconversion of catalytic species, *J. Am. Chem. Soc.* 131 (2009) 8410–8412.
- [4] W.B. Yao, Y.X. Zhang, X.Q. Jia, Z. Huang, Selective catalytic transfer dehydrogenation of alkanes and heterocycles by an iridium pincer complex, *Angew. Chem. Int. Ed.* 53 (2014) 1390–1394.
- [5] S. Muthaiah, S.H. Hong, Acceptorless and base-free dehydrogenation of alcohols and amines using ruthenium–hydride complexes, *Adv. Synth. Catal.* 354 (2012) 3045–3053.
- [6] S. Chakraborty, W.W. Brennessel, W.D. Jones, A molecular iron catalyst for the acceptorless dehydrogenation and hydrogenation of N-heterocycles, *J. Am. Chem. Soc.* 136 (2014) 8564–8567.
- [7] D. Jung, M.H. Kim, J. Kim, Cu-catalyzed aerobic oxidation of di-tert-butyl hydrazodicarboxylate to di-tert-butyl azodicarboxylate and its application on dehydrogenation of 1,2,3,4-tetrahydroquinolines under mild conditions, *Org. Lett.* 18 (2016) 6300–6303.
- [8] H. Choi, M.P. Doyle, Oxidation of secondary amines catalyzed by dirhodium caprolactamate, *Chem. Commun.* 38 (2007) 745–747.
- [9] Y. Wang, C.F. Li, J.H. Huang, External-ligand-free aerobic oxidation of N- and C-containing cyclic systems under Pd-catalyzed conditions, *Asian J. Org. Chem.* 6 (2017) 44–46.
- [10] C.L. Lou, S.H. Qin, S.C. Zhang, Z.N. Lv, A.M. Senan, Z.Q. Chen, G.C. Yin, Non-redox metal ions promoted oxidative dehydrogenation of saturated C–C bond by simple Pd(OAc)<sub>2</sub> catalyst, *Catal. Commun.* 90 (2017) 5–9.
- [11] W.Y. Zhou, P. Taboonpong, A.H. Aboo, L.J. Zhang, J. Jiang, J.L. Xiao, A convenient procedure for the oxidative dehydrogenation of N-heterocycles catalyzed by FeCl<sub>2</sub>/DMSO, *Synlett* 27 (2016) 1806–1809.
- [12] R.B. Xu, S. Chakraborty, H.M. Yuan, W.D. Jones, Acceptor less, reversible dehydrogenation and hydrogenation of N-heterocycles with a cobalt pincer catalyst, *ACS Catal.* 5 (2015) 6350–6354.
- [13] A. Nishinaga, T. Kondo, T. Matsuura, Oxygenation of cobalt(II) Schiff base complexes in alcohols, *Chem. Lett.* 14 (1985) 905–908.
- [14] K.H. He, F.F. Tan, C.Z. Zhou, G.J. Zhou, X.L. Yang, Y. Li, Acceptorless dehydrogenation of N-heterocycles by merging visible-light photoredox catalysis and cobalt catalysis, *Angew. Chem. Int. Ed.* 56 (2017) 3080–3084.
- [15] A.E. Wendlandt, S.S. Stahl, Modular o-Quinone catalyst system for dehydrogenation of tetrahydroquinolines under ambient conditions, *J. Am. Chem. Soc.* 136 (2014) 11910–11913.
- [16] K. Yamaguchi, N. Mizuno, Scope, kinetics, and mechanistic aspects of aerobic oxidations catalyzed by ruthenium supported on alumina, *Chem. Eur. J.* 9 (2003) 4353–4361.
- [17] F. Li, J. Chen, Q.H. Zhang, Y. Wang, Hydrogen ruthenium oxide supported on Co<sub>3</sub>O<sub>4</sub> as efficient catalyst for aerobic oxidation of amines, *Green Chem.* 10 (2008) 553–562.
- [18] K. Yamaguchi, N. Mizuno, Efficient heterogeneous aerobic oxidation of amines by a supported ruthenium catalyst, *Angew. Chem. Int. Ed.* 42 (2003) 1480–1483.
- [19] X.J. Cui, Y.H. Li, S. Bachmann, M. Scalone, A.E. Surkus, K. Junge, C. Topf, M. Beller, Synthesis and characterization of iron–nitrogen-doped graphene/core-shell catalysts: efficient oxidative dehydrogenation of N-heterocycles, *J. Am. Chem. Soc.* 137 (2015) 10652–10658.
- [20] D.V. Jawale, E. Gravel, N. Shah, V. Dauvois, H.Y. Li, I.N.N. Namboothiri, E. Doris, Cooperative dehydrogenation of N-heterocycles using a carbon nanotube–rhodium nanohybrid, *Chem. Eur. J.* 21 (2015) 7039–7042.
- [21] D. Damodara, R. Arundhathi, P.R. Likhari, Copper nanoparticles from copper aluminum hydrotalcite: an efficient catalyst for acceptor- and oxidant-free dehydrogenation of amines and alcohols, *Adv. Synth. Catal.* 356 (2014) 189–198.
- [22] Y. Mikami, K. Ebata, T. Mitsudome, T. Mizugaki, K. Jitsukawa, K. Kaneda, Reversible dehydrogenation–hydrogenation of tetrahydroquinoline–quinoline using a supported copper nanoparticle catalyst, *Heterocycles* 82 (2011) 1371–1377.
- [23] A.V. Iosub, S.S. Stahl, Catalytic aerobic dehydrogenation of nitrogen heterocycles using heterogeneous cobalt oxide supported on nitrogen-doped carbon, *Org. Lett.* 17 (2015) 4404–4407.
- [24] T. Hara, K. Mori, T. Mizugaki, K. Ebitani, K. Kaneda, Highly efficient dehydrogenation of indolines to indoles using hydroxyapatite-bound Pd catalyst, *Tetrahedron Lett.* 44 (2003) 6207–6210.
- [25] M.H. So, Y.G. Liu, C.M. Ho, C.M. Chen, Graphite-supported gold nanoparticles as efficient catalyst for aerobic oxidation of benzylic amines to imines and N-substituted 1,2,3,4-tetrahydroisoquinolines to amides: synthetic applications and mechanistic study, *Chem. Asian J.* 4 (2009) 1551–1561.
- [26] D.H. Ge, L. Hu, J.Q. Wang, X.M. Li, F.Q. Qi, J.M. Lu, X.Q. Cao, H.W. Gu, Reversible hydrogenation–oxidative dehydrogenation of quinolines over a highly active Pt nanowire catalyst under mild conditions, *ChemCatChem* 5 (2013) 2183–2186.
- [27] K. Mullick, S. Biswas, A.M. Angeles-Boza, S.L. Suib, Heterogeneous mesoporous manganese oxide catalyst for aerobic and additive-free oxidative aromatization of N-heterocycles, *Chem. Commun.* 53 (2017) 2256–2259.
- [28] J.Y. Zhang, S.Y. Chen, F.F. Chen, W.S. Xu, G.J. Deng, H. Gong, Dehydrogenation of N-heterocycles using graphene oxide as a versatile metal-free catalyst under air, *Adv. Synth. Catal.* 359 (2017) 2358–2363.
- [29] W.Y. Zhou, Q.Y. Tao, J.G. Pan, J. Liu, J.F. Qian, M.Y. He, Q. Chen, Effect of basicity on the catalytic properties of Ni-containing hydrotalcites in the aerobic oxidation of alcohol, *J. Mol. Catal. A Chem.* 425 (2016) 255–265.
- [30] W.Y. Zhou, P. Tian, F.A. Sun, M.Y. He, Q. Chen, Highly efficient transformation of alcohol to carbonyl compounds under a hybrid bifunctional catalyst originated from metalloporphyrins and hydrotalcite, *J. Catal.* 335 (2016) 105–116.

- [31] G.L. Fan, F. Li, D.G. Evans, X. Duan, Catalytic applications of layered double hydroxides: recent advances and perspectives, *Chem. Soc. Rev.* 43 (2014) 7040–7066.
- [32] D.G. Crivoi, A.M. Segarra, F. Medina, Highly selective multifunctional nanohybrid catalysts for the one-pot synthesis of alpha, beta-epoxy-chalcones, *J. Catal.* 334 (2016) 120–128.
- [33] J.F. Pang, M.Y. Zheng, L. He, L. Li, X.L. Pan, A.Q. Wang, X.D. Wang, T. Zhang, Upgrading ethanol to n-butanol over highly dispersed Ni-MgAlO catalysts, *J. Catal.* 344 (2016) 184–193.
- [34] J.T. Feng, Y.N. Liu, M. Yin, Y.F. He, J.Y. Zhao, J.H. Sun, D.Q. Li, Preparation and structure-property relationships of supported trimetallic PdAuAg catalysts for the selective hydrogenation of acetylene, *J. Catal.* 344 (2016) 854–864.
- [35] F.Z. Zhang, X. Xiang, F. Li, X. Duan, Layered double hydroxides as catalytic materials: recent development, *Catal. Surv. Asia* 12 (2008) 253–265.
- [36] X. Ning, Z. An, J. He, Remarkably efficient CoGa catalyst with uniformly dispersed and trapped structure for ethanol and higher alcohol synthesis from syngas, *J. Catal.* 340 (2016) 236–247.
- [37] T. Mitsudome, Y. Mikami, H. Funai, T. Mizugaki, K. Jitsukawa, K. Kaneda, Heterogeneous catalysis oxidant-free alcohol dehydrogenation using a reusable hydrotalcite-supported silver nanoparticle catalyst, *Angew. Chem. Int. Ed.* 47 (2008) 138–141.
- [38] K. Kon, W. Onodera, T. Toyao, K. Shimizu, Supported rhenium nanoparticle catalysts for acceptorless dehydrogenation of alcohols: structure-activity relationship and mechanistic studies, *Catal. Sci. Technol.* 6 (2016) 5864–5870.
- [39] N.L. Wang, J.E. Qiu, J. Wu, X. Yuan, K.Y. You, H.A. Luo, Microwave assisted synthesis of Sn-modified MgAlO as support for platinum catalyst in cyclohexane dehydrogenation to cyclohexene, *Appl. Catal. A Gen.* 516 (2016) 9–16.
- [40] Z.K. Zhao, Y.T. Dai, G.F. Ge, X.W. Guo, G.R. Wang, Facile simultaneous defect production and O, N-doping of carbon nanotubes with unexpected catalytic performance for clean and energy-saving production of styrene, *Green Chem.* 17 (2015) 3723–3727.
- [41] M. Ji, X.Y. Zhang, J.H. Wang, S.E. Park, Ethylbenzene dehydrogenation with CO<sub>2</sub> over Fe-doped MgAl<sub>2</sub>O<sub>4</sub> spinel catalysts: synergy effect between Fe<sup>2+</sup> and Fe<sup>3+</sup>, *J. Mol. Catal. A Chem.* 371 (2013) 36–41.
- [42] X.J. Jin, K. Taniguchi, K. Yamaguchi, K. Nozaki, N. Mizuno, A Ni-Mg-Al layered triple hydroxide-supported Pd catalyst for heterogeneous acceptorless dehydrogenative aromatization, *Chem. Commun.* 53 (2017) 5267–5270.
- [43] A. Nose, T. Kudo, Reduction of heterocyclic compounds. II. Reduction of heterocyclic compounds with sodium borohydride-transition metal salt systems, *Chem. Pharm. Bull.* 32 (1984) 2421–2425.
- [44] B.M. Choudhary, M.L. Kantam, A. Rahman, C.V. Reddy, K.K. Rao, The first example of activation of molecular oxygen by nickel in Ni-Al hydrotalcite: a novel protocol for the selective oxidation of alcohols, *Angew. Chem. Int. Ed. Engl.* 40 (2001) 763–766.
- [45] Z.L. Meng, Y.H. Zhang, Q. Zhang, X. Chen, L.P. Liu, S. Komarneni, F.Z. Lv, Novel synthesis of layered double hydroxides (LDHs) from zinc hydroxide, *Appl. Surf. Sci.* 396 (2017) 799–803.
- [46] A. Coelho, O. Micali, P. Eleni, G. Roberto, D.-S. João, C. Thoméo, M. Boscolo, Mixed metal oxides from sucrose and cornstarch templated hydrotalcite-like LDHs as catalysts for ethyl biodiesel synthesis, *Appl. Catal. A Gen.* 532 (2017) 32–39.
- [47] Q.H. Tang, C.M. Wu, R. Qiao, Y.T. Chen, Y.H. Yang, Catalytic performances of Mn-Ni mixed hydroxide catalysts in liquid-phase benzyl alcohol oxidation using molecular oxygen, *Appl. Catal. A Gen.* 403 (2011) 136–141.
- [48] J.M. Fernandez, C. Barriga, M.A. Ulibarri, F.M. Labajos, V. Rives, Preparation and thermal stability of manganese-containing hydrotalcite, [Mg<sub>0.75</sub>Mn<sub>0.04</sub>Mn<sub>0.21</sub>(OH)<sub>2</sub>](CO<sub>3</sub>)<sub>0.11</sub>·nH<sub>2</sub>O, *J. Mater. Chem.* 4 (1994) 1117–1121.
- [49] P. Benito, F.M. Labajos, V. Rives, Microwave-treated layered double hydroxides containing Ni<sup>2+</sup> and Al<sup>3+</sup>: the effect of added Zn<sup>2+</sup>, *J. Solid State Chem.* 179 (2006) 3784–3797.
- [50] E.M. Seftel, M. Puscasu, M. Mertens, P. Cool, G. Carja, Photo-responsive behavior of  $\gamma$ -Fe<sub>2</sub>O<sub>3</sub> NPs embedded into ZnAlFe-LDH matrices and their catalytic efficiency in wastewater remediation, *Catal. Today* 252 (2015) 7–13.
- [51] S. Miyata, The syntheses of hydrotalcite-like compounds and their structures and physico-chemical properties I: The systems Mg<sup>2+</sup>-Al<sup>3+</sup>-NO<sub>3</sub>, Mg<sup>2+</sup>-Al<sup>3+</sup>-Cl<sup>-</sup>, Mg<sup>2+</sup>-Al<sup>3+</sup>-ClO<sub>4</sub><sup>-</sup>, Ni<sup>2+</sup>-Al<sup>3+</sup>-Cl-and Zn<sup>2+</sup>-Al<sup>3+</sup>-Cl, *Clays Clay Miner.* 23 (1975) 369–375.
- [52] B. Dragoi, A. Ungureanu, A. Chiriac, C. Ciotonea, C. Rudolf, S. Royer, E. Dumitriu, Structural and catalytic properties of mono- and bimetallic nickel-copper nanoparticles derived from MgNi(Cu)Al-LDHs under reductive conditions, *Appl. Catal. A Gen.* 504 (2015) 92–102.
- [53] P. Kowalik, M. Konkol, M. Kondracka, W. Próchniak, R. Bicki, P. Wiercioch, Memory effect of the CuZnAl-LDH derived catalyst precursor-in situ XRD studies, *Appl. Catal. A Gen.* 464 (2013) 339–347.
- [54] H. Huang, J. Huang, Y.M. Liu, H.Y. He, Y. Cao, K.N. Fan, Graphite oxide as an efficient and durable metal-free catalyst for aerobic oxidative coupling of amines to imines, *Green Chem.* 14 (2012) 930–934.
- [55] Z.H. Xiao, Insight into the Meerwein-Ponndorf-Verley reduction of cinnamaldehyde over MgAl oxides catalysts, *Mol. Catal.* 436 (2017) 1–9.
- [56] H.T. Kang, K. Lv, S.L. Yuan, Synthesis, characterization, and SO<sub>2</sub> removal capacity of MnMgAlFe mixed oxides derived from hydrotalcite-like compounds, *Appl. Clay Sci.* 72 (2013) 184–190.
- [57] X.F. Zhao, L. Wang, X. Xu, X.D. Lei, S.L. Xu, F.Z. Zhang, Fabrication and photocatalytic properties of novel ZnO/ZnAl<sub>2</sub>O<sub>4</sub> nanocomposite with ZnAl<sub>2</sub>O<sub>4</sub> dispersed inside ZnO network, *AIChE J.* 58 (2012) 573–582.
- [58] S. Velu, N. Shah, T.M. Jyothi, S. Sivasanker, Effect of manganese substitution on the physicochemical properties and catalytic toluene oxidation activities of Mg-Al layered double hydroxides, *Micropor. Mesopor. Mater.* 33 (1999) 61–75.
- [59] S.T. Oyama, X.M. Zhang, J.Q. Lu, Y.F. Gu, T. Fujitani, Epoxidation of propylene with H<sub>2</sub> and O<sub>2</sub> in the explosive regime in a packed-bed catalytic membrane reactor, *J. Catal.* 257 (2008) 1–4.
- [60] S. Mukherjee, M.A. Vannice, Solvent effects in liquid-phase reactions: I. Activity and selectivity during citral hydrogenation on Pt/SiO<sub>2</sub> and evaluation of mass transfer effects, *J. Catal.* 243 (2006) 108–130.
- [61] J. Zhu, M. Li, M.H. Lu, J.J. Zhu, Effect of structural properties on catalytic performance in citral selective hydrogenation over carbon-titania composite supported Pd catalyst, *Catal. Sci. Technol.* 3 (2013) 737–744.
- [62] R.S. Jayashree, P.V. Kamath, Layered double hydroxides of Ni with Cr and Mn as candidate electrode materials for alkaline secondary cells, *J. Power Sources* 107 (2002) 120–124.
- [63] K. Shaju, G.S. Rao, B. Chowdari, Lithiated O<sub>2</sub> phase, Li<sub>(2/3)+x</sub>(Co<sub>0.15</sub>Mn<sub>0.85</sub>)O<sub>2</sub> as cathode for Li-ion batteries, *Solid State Ionics* 152–153 (2002) 69–81.
- [64] Q. Shen, L.Y. Zhang, N.N. Sun, H. Wang, L.S. Zhong, C. He, W. Wei, Y.H. Sun, Hollow MnOx-CeO<sub>2</sub> mixed oxides as highly efficient catalysts in NO oxidation, *Chem. Eng. J.* 322 (2017) 46–55.
- [65] D.A. Peña, B.S. Uphade, P.G. Smirniotis, TiO<sub>2</sub>-supported metal oxide catalysts for low-temperature selective catalytic reduction of NO with NH<sub>3</sub>: I. Evaluation and characterization of first row transition metals, *J. Catal.* 221 (2004) 421–431.
- [66] J. Zhao, J. Chen, S. Xu, M. Shao, Q. Zhang, F. Wei, J. Ma, M. Wei, D.G. Evans, X. Duan, Hierarchical NiMn layered double hydroxide/carbon nanotubes architecture with superb energy density for flexible supercapacitors, *Adv. Funct. Mater.* 24 (2014) 2938–2946.
- [67] M. Li, F. Liu, J.P. Cheng, J. Ying, X.B. Zhang, Enhanced performance of nickel-aluminum layered double hydroxide nanosheets/carbon nanotubes composite for super capacitor and asymmetric capacitor, *J. Alloys Compd.* 635 (2015) 225–232.
- [68] D. Talwar, A. Gonzalez-de-Castro, H.Y. Li, J.L. Xiao, Regioselective acceptorless dehydrogenative coupling of N-heterocycles toward functionalized quinolines, phenanthrolines, and indoles, *Angew. Chem. Int. Ed.* 54 (2015) 5223–5227.